A HEAT SOURCE MODEL TO SIMULATE WELDING PROCESSES WITH MAGNETIC DEFLECTION

Fernanda Mazuco Clain, fernandaclain@furg.br
Paulo Roberto de Freitas Teixeira @gmail.com
Universidade Federal do Rio Grande – FURG, Av. Itália km 8, Rio Grande, Brazil

Douglas Bezerra de Araújo, douglas_ba@yahoo.com
Universidade Federal de Uberlândia – UFU, Av. João Naves de Ávila, 2121, Uberlândia, Brazil

Abstract. *Welding with weaving has been widely used for improving process efficiency and distribution of heat input. The technique of weaving by magnetic deflection of the arc was developed a few years ago to enable the oscillation of the weld pool, thus, causing grain refinement and improving the properties on the welded joint. The numerical simulation of this type of process is complex because of the influence of the magnetic field on the electric arc, a fact that has not been taken into consideration by standard welding processes. This paper aims to describe a numerical heat source model, including the effects of arc deflection on bead-on-plate GTAW process. Numerical simulations are carried out considering magnectic deflected and non-deflected arcs throughout the welding process. Results are compared to the ones obtained experimentally. Temperatures at three different points on the backside of the plates (two out of the center line and one in the center line of welding) and weld pools of SAE 1020 3.2-mm thick steel plates are analyzed. Results obtained by numerical simulations are close to the experimental ones. In the case of welding with arc deflection, temperatures of thermocouples placed on the side in which the arc was deflected and on the center are very similar. Weld penetration is higher in the welding without the arc deflection than in the welding with arc deflection. The asymmetry of the fusion zone shape for welding with arc deflection was captured by numerical simulation.*
Keywords*: heat source model, numerical simulation, GTAW process, magnetic arc deflection*

1. INTRODUCTION

Welding with weaving is a widespread process in which the torch movement enables the deposit of wider weld bead with lower penetration. The weaving technique by magnetic deflection of the arc has recently been developed to enable the oscillation of the weld pool and, consequently, has caused grain refinement and has improved the properties on the welded joint.

Experiments carried out by Sudaresn and Ram (1999) with titanium alloy showed that the magnetic deflection applied to TIG welding processes causes significant grain refinement. Similarly, Kumar et al. (2008) and Lim et al. (2010) also reported the increase in the grain refinement when magnetic deflection was used and, thus, the increase in mechanical strength in alloys under investigation.

Other researchers used this technique to study the geometry of the weld bead. Kang and Na (2003) applied the transversal magnetic deflection to MIG/MAG narrow gap welding and they obtained good uniformity and penetration in both sides of the groove. Bracarense and Soares (2010) and Soares (2010) investigated the magnetic deflection in low carbon steel by the MIG/MAG process in root passes. They obtained more control of welding pool and root reinforcement, more metal transfer process stability and low weld spatter.

Numerical simulation has been an alternative to investigate in detail the effects of the arc deflection on the heat input distribution of the welding plate, since the increase in the computer capacity has made it quick and inexpensive in the last years. The finite element method (FEM) has been widely used to deal with welding process problems which involve thermal, metallurgical and mechanical phenomena.

Nowadays, there are models to represent the heat input distribution in the welding when the torch is perpendicular to the plate planes (Hu et al., 2006), but there are few proposals for cases with arc deflection, such as those presented in magnetic weaving. Hongyuan et al. (2005), for example, developed a numerical model of heat input source applied to cases in which magnetic arc deflection is caused by the magnetic interaction in twin wire GMAW welding. In this numerical model, the magnetic arc deflection is caused by the torch inclination in relation to the welding plane by employing a double ellipsoid heat source model.

The aim of this study is to develop and validate a heat input source model to simulate the magnetic arc deflection in a weld bead in autogean GTAW process. The welding process in steel plates 3.2-mm thick (SAE 1020) are simulated on deflected and non-deflected arcs by ANSYS Multiphysics software®. Temperatures at three positions on the backside of the plates and dimensions of the fusion zone are compared with those obtained experimentally.

2. THERMAL ANALYSIS OF THE WELDING PROCESS

2.1 Governing equation and boundary conditions

The thermal field is governed by the heat conduction equation, given by

$$\frac{\partial}{\partial x}\left(k(T)\frac{\partial T}{\partial x}\right)+\frac{\partial}{\partial y}\left(k(T)\frac{\partial T}{\partial y}\right)+\frac{\partial}{\partial z}\left(k(T)\frac{\partial T}{\partial z}\right)+Q_V=\rho(T)C_p(T)\frac{\partial T}{\partial t} \quad (1)$$

where T is the temperature, $k(T)$ is the thermal conductivity, $\rho(T)$ is the specific mass, $Cp(T)$ is the specific heat and Q_V is the rate at which energy is generated per unit volume of the medium (in this study, Q_V is null).

A phase change with melting and solidification is involved in the welding process. Enthalpy methods are some of several techniques to deal with this type of problem (Hu and Argyropoulos, 1996). The essential feature of basic enthalpy methods is that the evolution of the latent heat is accounted for the enthalpy as well as the relation between enthalpy and temperature. These methods are based on the heat conduction equation expressed in function of the enthalpy (H) as follows:

$$\frac{\partial}{\partial x}\left(k(T)\frac{\partial T}{\partial x}\right)+\frac{\partial}{\partial y}\left(k(T)\frac{\partial T}{\partial y}\right)+\frac{\partial}{\partial z}\left(k(T)\frac{\partial T}{\partial z}\right)=\frac{\partial[H(T)]}{\partial t} \quad (2)$$

where Q_V is intentionally omitted and enthalpy H is the integral of the heat capacity with respect to temperature:

$$H=\int \rho(T)C_p(T)dT \quad (3)$$

The thermodynamic boundary conditions on the external surfaces of the solid comprise heat transfer for convection and radiation. The heat flow density for convection (q_c) in the environment gas or liquid is given by Newton's heat transfer law:

$$q_c=h_c(T-T_0) \quad (4)$$

where T is the temperature of the external surface, T_0 is the temperature of gas or liquid and h_c is the coefficient of convective heat transfer. This coefficient depends on the convection conditions on the solid surface, besides the properties of the surface and the environment.

The heat flow density for radiation q_r is governed by the Stefan-Boltzmann law, as follows

$$q_r=\varepsilon_r\sigma_r(T^4-T_0^4) \quad (5)$$

where ε_r is the emissivity of the material surface and σ_r is the Stefan-Boltzman constant.

2.2 Heat source models

In this study, the heat of the welding arc is modeled by a traveling two-dimensional distribution of a heat source with a Gaussian distribution. Therefore, the heat flux distribution on the surface of the solid is related to the radial position r (whose origin is the arc center). The heat flux distribution considering the torch perpendicular to the plates is given by (Goldak, and Akhlaghi, 2005)

$$q(r)=q_m e^{-(r^2/2\sigma^2)} \quad (6)$$

where $q(r)$ is the surface flux at radius r, $q_m=\eta UI/2\pi\sigma^2$ is the maximum heat flux in the source center, η is the efficiency coefficient, U is the voltage, I is the current and σ is the radial distance from the center. The surface flux is reduced by 5% when the $r=2.45\sigma$ and it is practically null when $r=3\sigma$ (Goldak, and Akhlaghi, 2005).

A new heat source model is necessary to reproduce cases which the arc is deflected. Figure 1 shows a sketch of the proposal of this study for these cases. The arc inclination (θ) displaces the position of the source center and only the perpendicular component of the heat flux is considered to input into the plates. Therefore, the maximum heat flux in the source center, in this case, is

$$q_m=\left(\eta UI/2\pi\sigma^2\right)\cos\theta \quad (7)$$

Moreover, the radius r is modified according to the side of the point on the plate surface in relation to the source center. Figure 1 shows, for an x transversal position of the point, the ones that must be considered in the heat source equation, x' and x'', which are positions at left and right sides, respectively, determined by the follow expressions:

$$x'=x\cos\theta;\quad x''=x/\cos\theta \quad (2)$$

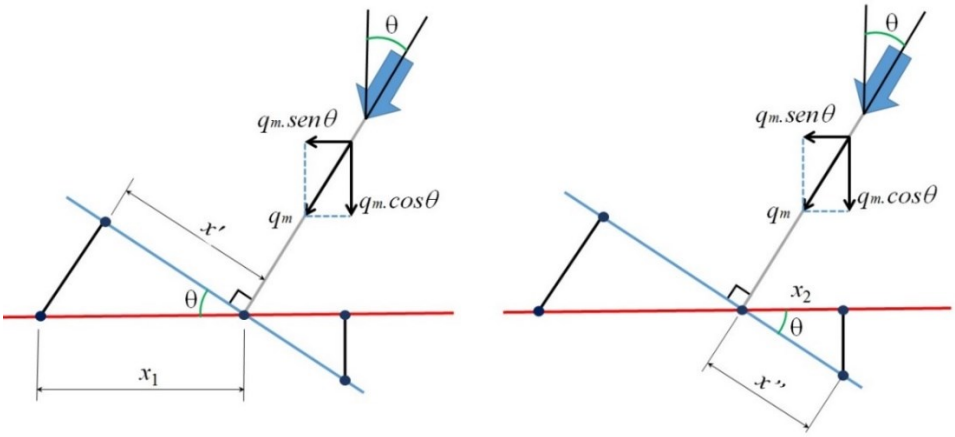

Figure 1. Sketch of the heat flux into the plates.

Thus, the radius at left and right sides to be used in the heat source are calculated considering these modified coordinates (Eq. (6)) and given by:

$$r' = \sqrt{((x')^2 + z^2)}; \quad r'' = \sqrt{((x'')^2 + z^2)} \tag{3}$$

3. CASE STUDY AND MATHEMATICAL MODEL

The case study is an autogean bead-on-plate GTAW process which is carried out at laboratory of research in welding engineering (LAPES – FURG). The plates are 3.2 mm thick, 200 mm long, 100 mm wide and their material is the SAE 1020 steel. The welding is conducted by using the 6-axis weld robot Motoman HP20D (repeatability = ±0,06 mm), with an welding speed 0.0025 m/s (15 cm/min), and the Power Wave® 455M/STT Advanced Process Welder. The distance from the contact tip to the plate surface is 6 mm and the argon shielding gas with flow rate of 2.17x10-4 m3/s (13 l/min) is used. The mean current and voltage are 100 A and 15 V, respectively.

Two experiments are carried out: (b) without arc deflection and (c) with magnetic arc deflection (see Fig. 2). Temperatures at three points are measured by thermocouples (type K) located at the opposite face of the weld (Fig. 2) at the middle of the plates in longitudinal direction; one is located at the center line and the others are 5 mm from the center line. They are attached to the metal plate with the use of a capacitive discharge. The data acquisition measurement system is the NI9211 model of National Instruments (accuracy < 0.07K) with 3.5 sample/s/ch and resolution of 24 bits. The transversal section of the fusion zone is obtained by cutting the welded plate which receives a chemical attack with nital 3% to the macrography analysis.

A solenoid is connected to the torch to induce a magnetic field in the arc and to cause its transversal deflection (Fig. 2a). The deflection direction (right or left sides) and the arc inclination depend on the voltage applied to the solenoid; in this case, the voltage is 4 V that causes an arc inclination of 25º.

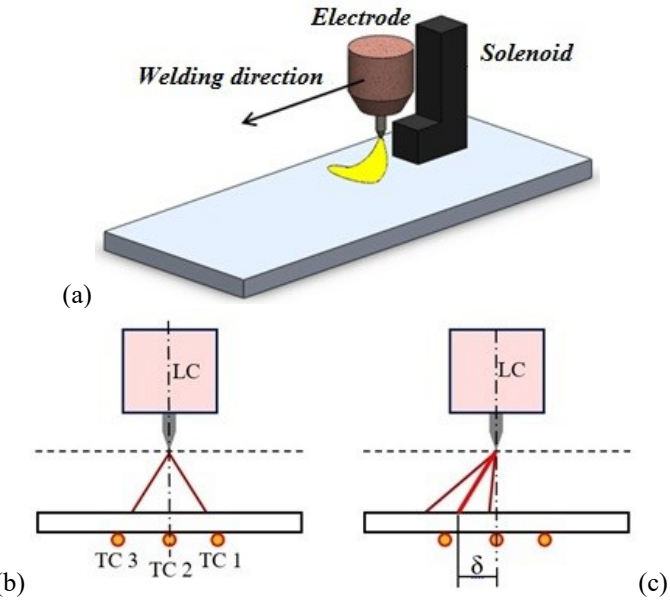

Figure 2. Sketch of the welding with magnetic deflection (a) and thermocouple positions for non-deflected (b) and deflected arcs (c).

Numerical simulations are carried out by using ANSYS Multiphysics®, which solves the transient thermal equation based on the FEM. Hexahedral elements with eight nodes and surface elements to impose the convection and radiation conditions are employed. The mapped mesh has 55275 nodes and 43200 elements, as shown in Fig. 3. In the central region up to 0.015 m from the welding line, to both sides, the element size is 0.001 m while out of this zone, it is 0.002 mm.

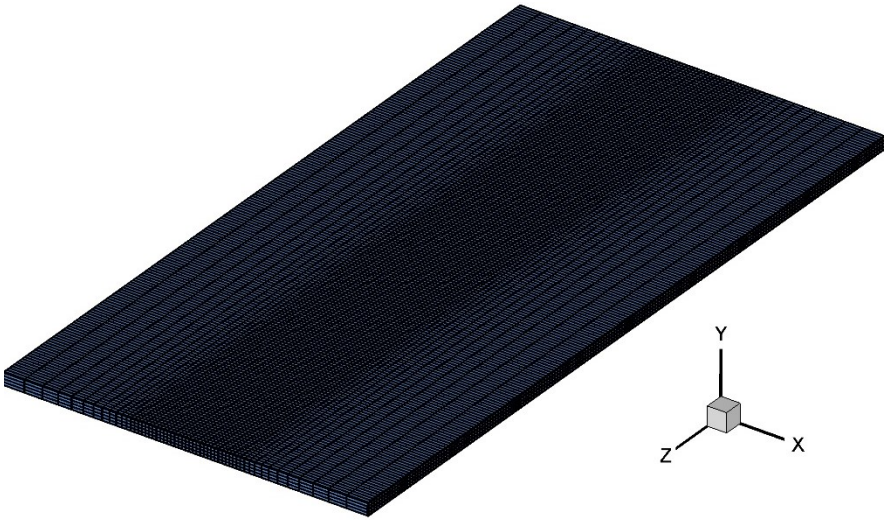

Figure 3 – Mapped mesh

The moving Gaussian heat source model is used to impose the heat flux on welding surface. The radial distance from the center ($\sigma = 2.4$ mm) and the efficiency ($\eta = 57\%$) are set, in the validation process, to reach the best temperature curve adjustment and the fusion zone in relation to the experimental ones. This efficiency is according to the range studied by Arevalo and Villarinho (2012). Thermal properties of the steel SAE 1020 used in numerical simulations are temperature dependent. Figure 4 shows the relation between enthalpy (H), thermal conductivity (k) and specific mass (ρ) with temperature. Emissivity is $\varepsilon_r = 0.8$ and the coefficient of convective heat transfer is $hc = 15$ W/m^2 °C.

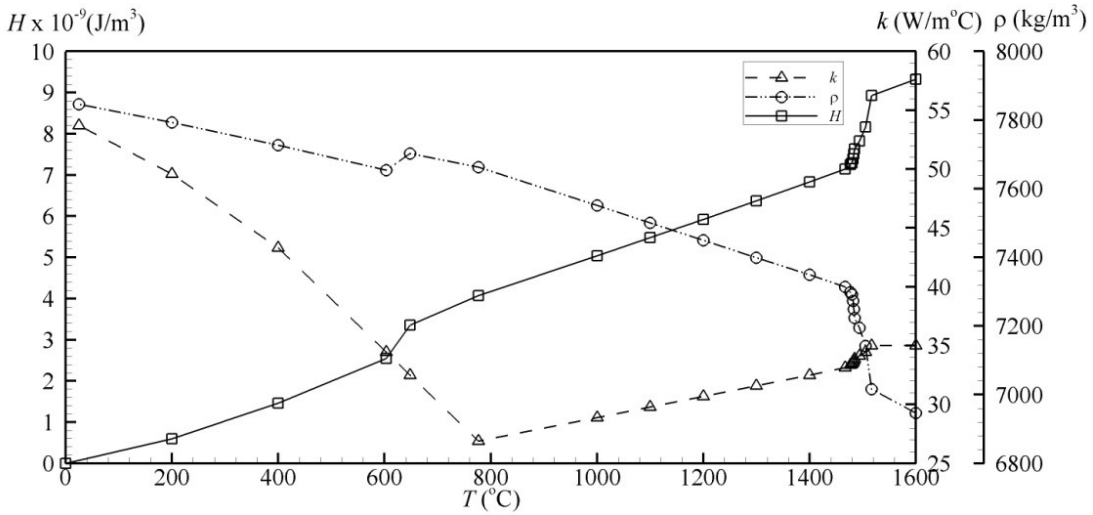

Figure 4. Thermal properties of steel SAE 1020

4. RESULTS

In this Section, numerical results considering deflected and non-deflected arcs are compared with experimental ones. Images of the electric arc for the two cases are shown in Fig. 5. The distorted shape of the deflected arc shows the influence of the magnetic field on the behavior of the arc and, consequently, on its heat input into the plate.

Temperature distribution on the plate at three instants along the welding process for non-deflected arc is shown in Fig. 6. As expected, high temperatures are concentrated around the heat source as it moves. Also, rear zones have higher temperatures in relation to other zones along the welding.

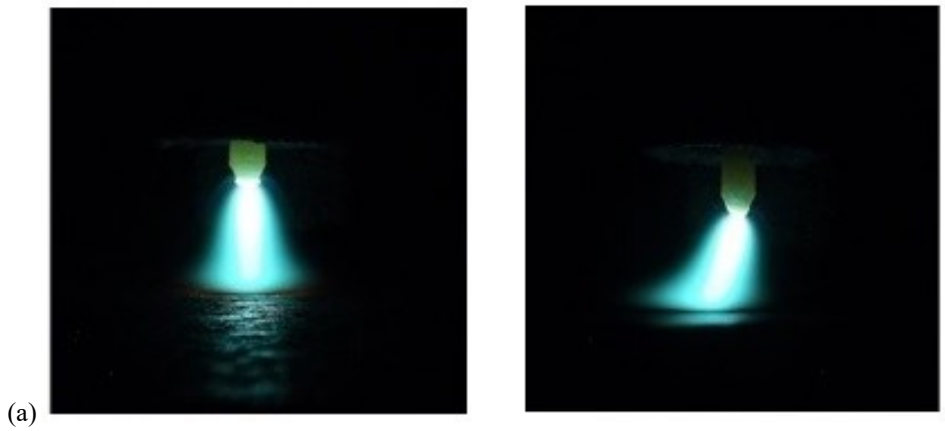

Figure 5. Electric arc (a) without and (b) with magnetic deflection.

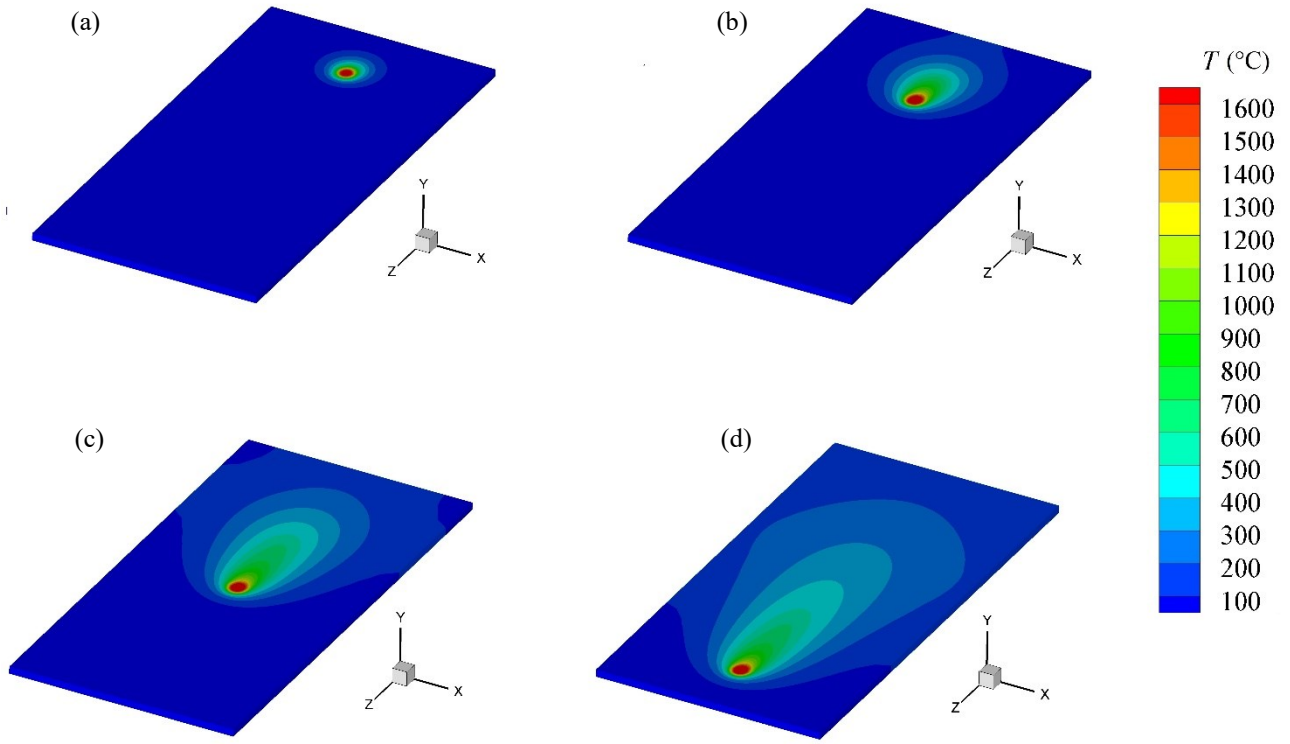

Figure 6. Temperature distribution at three instants along the welding for non-deflected arc: (a) 2.8 s, (b) 12 s, (c) 32 s and (d) 60 s.

Figure 7 shows the thermal cycles of the two cases: (a) non-deflected and (b) deflected arc. For the first case (non-deflected arc), the temperature at TC2 (in welding center line) is higher than at TC1 and TC3, that are 5 mm far from the center line, as shown in Fig. 2. Additionally, temperature curves at TC1 and TC3 are very similar, duo to the expected symmetry of the welding behavior. Moreover, an asymmetry is observed for the second case (deflected arc). In this case, the temperature on the same side of the arc deflection direction (the left side of the torch – TC3 in Fig. 2) is higher than that on another side (TC1) and similar to the temperature at the center line (TC2).

In general, numerical results are in good agreement with experimental ones. For the non-deflected case, differences of temperature peaks are 14%, 9% and 5%, for TC1, TC2 and TC3, respectively, while for the deflected case are 3% for TC1, 2% for TC2 and 8% for TC3. The slope of the temperature curve after the peak represents the cooling rate, which is related to the heat transfer of the plate to the environment. In this case, the numerically obtained cooling rates are in good agreement with the experimental results. This fact leads to the conclusion that boundary conditions, the coefficient of convection heat transfer and radiation conditions are well represented by the simulations. Temperature curves obtained numerically and experimentally, for deflected case, are very similar at three positions. These results show the applicability of the proposal heat source model to the magnetic arc deflection.

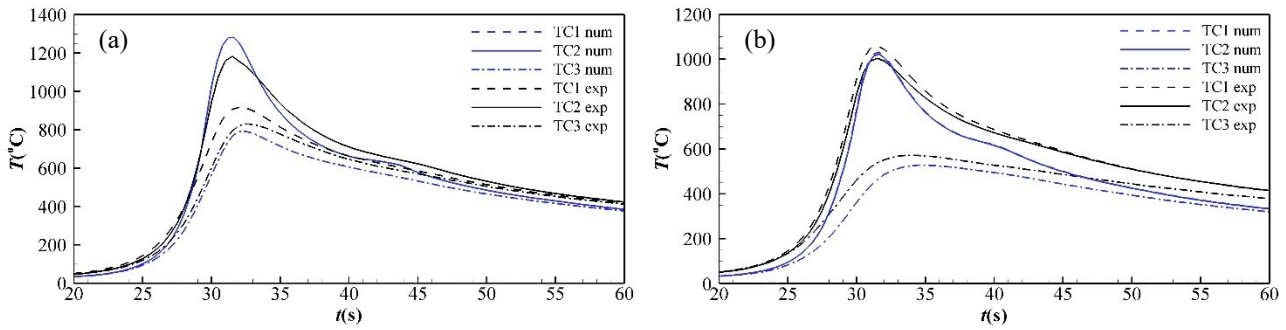

Figure 7. Thermal cycles at TC1, TC2 and TC3 for non-deflected (a) and deflected arcs (b).

Figure 8 shows the weld pool zones numerically and experimentally obtained for non-deflected (a) and deflected arcs (b). The penetrated depth (1.6 mm) in the non-deflected arc is higher than that in the deflected arc (1.1 mm), while they have the same bead widths (4.5 mm). The welding pool is practically symmetric for non-deflected arc and there is an expected asymmetry for the deflected arc.

In general, numerical results reproduce adequately the shapes of the fusion zones. Penetrated depths obtained numerically are very close to the experimental ones for both cases, with difference of 5% and 6% for non-deflected and deflected arcs, respectively, while bead widths are larger, with difference of 28% and 10% for non-deflected and deflected arcs. The asymmetry of the weld pool zone in the deflected arc is captured by the model, as shown in Fig. 7b.

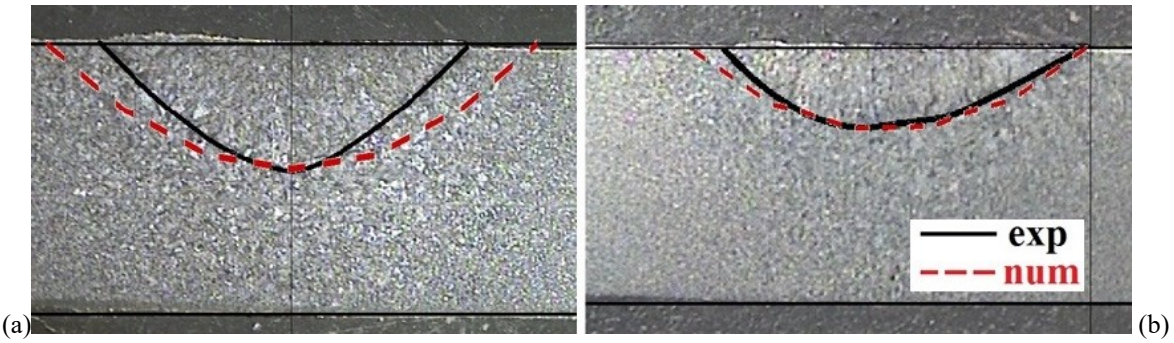

(a) (b)

Figure 8. Weld pools obtained experimentally and numerically for non-deflected (a) and deflected arcs (b).

5. CONCLUSION

This paper described a numerical heat source model to include the effects of arc deflection duo to the presence of a magnetic field. A modified formulation of the Gaussian heat source distribution model was proposed for numerical simulations by using ANSYSMultiphysics® and their results were compared to the ones obtained experimentally. A bead-on-plate GTAW process applied to a SAE 1020 3.2-mm thick steel plate was analyzed. Temperatures at three different points on the backside of the plate (two out of the center line and one in the center line of welding) showed that numerical results were close to the experimental ones in both cases: non-deflected and deflected arc. For cases with deflected arc by the magnetic field, temperatures on the same side of the arc deflection and at the welding center line were very similar. Weld pools were adequately reproduced by the simulations. The penetrated depths obtained numerically were very close to the experimental ones for both cases, while the bead widths were larger. The asymmetry of the weld pool zone in the deflected arc was captured by the model.

This study shows the capacity of the proposal heat source model to deal with welding subjected to the magnetic deflection and, therefore, this heat source model is able to simulate welding with weaving. However, the calibration of the Gaussian heat source is restricting duo to its limited degrees of freedom. This disadvantage can be circumvent by using volumetric heat sources, although the calibration process is more difficult because their greater degrees of freedom.

6. REFERENCES

Arevalo, H. D. H., Vilarinho, L. O. Desenvolvimento e Avaliação de Calorímetros por Nitrogênio Líquido e Fluxo Contínuo para Medição de Aporte Térmico. Soldagem e Inspeção, Vol.17, Nº. 3, p.236-250. São Paulo, 2012.

Bracarense, A. Q.; Soares, L. F. Uso de Oscilação Magnética do Arco Elétrico para Preenchimento de Passe de Raiz em Juntas Chanfradas de Aços Baixo Carbono Através do Processo GMAW. In: VI CONEM, 2010, Campina Grande, PB, Brasil.

Goldak, J. A.; Akhlaghi, M. Computational welding mechanics. Springer, 2005.

Hongyuan F., Qingguo M., Wenli X., Shude J. New general double ellipsoid heat source model. Science and Technology of Welding and Joining. Vol 10, n. 3, p. 361-368, 2005.

Hu J. F., Yang J. G., Fang H. Y., Li G. M., Zhang Y. Numerical simulation on temperature and stress fields of welding with weaving. Science And Technology Of Welding And Joining. Vol 11, n. 3, p. 358-365, 2006.

Hu H., Argyropoulos S.A. (1996) Mathematical modeling of solidification and melting: a review. *Modelling and Simulation in Materials Science and Engineering* 4:371-396.

Kang, Y. H.; Na S. J. Characteristics of Welding and Arc Signal in Narrow Groove Gas Metal Arc Welding Using Electromagnetic Arc Oscillation: Experiments produce optimum parameters for obtaining uniform and sufficient groove face penetration. Welding Journal. p. 93-S-99-S, May, 2003.

Kang, Y. H.; Na S. J. A Study on the Modeling of Magnetic Arc Deflection and Dynamic Analysis. Welding Journal. January 2002.

Kumar, A.; Shailesh, P.; Sundarrajan, S. Optimization of magnetic arc oscillation process parameters on mechanical properties of AA 5456 Aluminum alloy weldments. Materials and Design. p. 1094-1913. 2008.

Lancaster, J. F. The Physics of Welding. 2. ed. Oxford: Pergamon Press, 1986. 340p.

Lim, Y. C. et al. Effect of magnetic stirring on grain structure refinement: Part 2 – Nickel alloy weld overlays. Science and Technology of Welding and Joining. v. 15, n. 5, p.400-406, 2010.

Soares, L. F. Uso de Oscilação Magnética do Arco Elétrico para Preenchimento do Passe de Raiz em Juntas Chanfradas de Aço Baixo Carbono com o Processo GMAW. Universidade Federal de Minas Gerais, 2010.

Sundaresan, S.; Ram, G. D. J. Use of magnetic arc oscillation for grain refinement of gas tungsten arc welds in α–β titanium alloys. Science and Technology of Welding and Joining, v. 4, n. 3, p.151-160, 1999.

Rosenthal, D. Mathematical theory of heat distribution during welding and cutting. Welding Journal, 1941.

7. RESPONSIBILITY NOTICE

The authors are the only responsible for the printed material included in this paper.